

Connection between blazes from gratings and enhancements from random rough surfaces

M. Nieto-Vesperinas and J. M. Soto-Crespo

Instituto de Optica, Consejo Superior de Investigaciones Científicas, Serrano 121, E-28006 Madrid, Spain

(Received 8 July 1988; revised manuscript received 17 October 1988)

We show that the blaze effect for the antispecular orders from deep reflection gratings is intimately connected with the enhancement of the mean backscattered intensity from deeply rough random surfaces. We also prove that when the illuminated structure has a center of symmetry then the intensity in the specular direction can also be enhanced.

I. INTRODUCTION

In a previous paper¹ we showed that the light-diffracted intensities from perfectly conducting deep reflection gratings have a remarkable tendency to be enhanced either in the specular or in any of the antispecular orders. The curves of the diffracted intensities versus grating depth, for a certain profile and a given incidence angle θ_0 , exhibit a characteristic oscillatory behavior (cf. Ref. 1 and references therein) whose amplitudes are markedly larger for the specular or the antispecular (if it exits at that angle of incidence). Thus, although it is possible to devise a particular grating with blaze in a chosen order, statistically, over a set of profiles *a priori* given, are the specular, or the antispecular diffraction orders, those with the highest probability of enhancement.

Blaze of antispecular intensities under a particular incidence angle and for a certain profile in the Littrow mount is a well-known phenomenon.^{2,3} However, what we show here is the tendency of deep reflection gratings to present blaze in all antispecular orders (or in the specular, alternatively).

The gratings studied in Ref. 1 were sinusoidal or combinations of two sinusoids. We hinted there, without giving a proof, that the aforementioned enhancements might be intimately connected with the phenomenon of enhanced backscattering from deep random rough surfaces.⁴⁻⁶ Nevertheless, the question of why on the average over many samples the antispecular is dominant over the specular was left unanswered in Ref. 1. The gratings studied in Ref. 1 were, however, symmetric. The first purpose in this paper is to show that this property is the determinant for the enhancement of the specular.

It appears at first sight to be an analogy between the enhanced backscattering from random rough surfaces and the effect of photon localization in random media (a brief review with references on this phenomenon may be found in Ref. 7). In fact, a simple picture, based on geometrical optics with \mathbf{k} vectors, of the way in which multiple reflections at a rough surface may lead to backscattering enhancements was drawn by the authors of Refs. 4 and 5. This argument is analogous to the so-called coherent backscattering process used in some of the references quoted in Ref. 7 (in particular, in Refs. 8

and 9). However, the question of whether or not this backscattering enhancement from very rough random surfaces is indeed similar in nature to the one due to photon localization in random media remains still open.¹⁰

The second main task of this work is to prove the intimate connection between the high probability of blaze in the antispecular intensity diffracted from deep reflection gratings, as pointed out in Ref. 1, and the effect of enhanced backscattering from very rough random surfaces. In order to carry this out, we shall work with gratings of arbitrary profile and a great deal of Fourier coefficients, constructed in the following manner: We computer generate a random series of numbers with zero mean, normal statistics, and rms σ and correlation length T ; the correlation function being Gaussian. (We believe, however, that this particular statistics and correlation function are not essential for our purpose.) Then, an interval of length a (with typically 220 sampling points) is extracted from that series. The grating $z=D(x)$ of period a is subsequently simulated by periodically repeating this interval of length a . Obviously, a random surface would be the limiting case when a becomes very large. (See in this connection the classical work of Ref. 11.)

II. NUMERICAL RESULTS

Calculations of the diffracted intensities are made for incident plane waves, linearly polarized under s or p polarization, interacting with the interface $z=D(x)$ that separates a vacuum from a perfect conductor. These intensities are

$$\begin{Bmatrix} I_n^s \\ I_n^p \end{Bmatrix} = \frac{k_{nz}}{k_{0z}} \begin{Bmatrix} |A_n|^2 \\ |B_n|^2 \end{Bmatrix}, \quad (1)$$

A_n and B_n the diffracted amplitudes corresponding to s and p waves, respectively. The induced current densities, necessary to obtain A_n and B_n , are calculated from the extinction theorem^{12,13} according to the method of Ref. 1.

In Eq. (1) k_{0z} and k_{nz} are the z components of the incident and n th-diffracted wave vectors, respectively. Therefore

$$K_0^2 + k_{0z}^2 = k^2, \quad (2a)$$

$$K_n^2 + k_{nz}^2 = k^2, \quad k = 2\pi/\lambda \quad (2b)$$

and

$$K_n = K_0 + 2\pi n/a. \quad (3)$$

The diffracted intensities should satisfy the unitarity condition

$$\sum_{n=-\infty}^{\infty} I_n^{(s,p)} = 1. \quad (4)$$

Equation (4) is used as a criterion of numerical accuracy of our calculations.

All results shown in this work are for *s* polarization, unless explicitly stated otherwise. It should be pointed out, however, that no significant differences were observed between the results from *s* and *p* polarization for large depths characterized by the rms σ (in agreement with Ref. 14). Calculations have been done obtaining errors in the unitarity no larger than 3% and usually smaller than 1%.

For a given period a , 200 samples (i.e., gratings) of the same period are simulated. Each grating is built by choosing a different interval of the same random series of given σ and T according to the procedure described above. The distribution of diffracted intensities is obtained from each grating. Then the average of the resulting 200 intensity patterns is performed, thus giving a distribution of orders whose envelope will become close to the mean scattered intensity from 200 samples of a random surface of the same parameters σ and T , when a becomes large. The statistical bias of the mean scattered intensities produced slightly asymmetric diffraction patterns at incidence angle $\theta_0 = 0^\circ$ that were artificially symmetrized at this particular angle of incidence by averaging every two intensities at θ and $-\theta$.

Figure 1 shows the mean diffracted intensities from 200 gratings of period $a = 1.78\lambda$ extracted from a random series with $T = 0.24\lambda$ and $\sigma = 0.5\lambda$ and 0.6λ , at $\theta_0 = 0^\circ$, 16° , 46° , and 57° . As seen, on the average over 200 profiles, the antispecular intensity is enhanced at those angles of incidence at which it exists. At a large incidence angle, e.g., $\theta_0 = 46^\circ$, the specular intensity is higher; this is not only due to the nonexistence of antispecular order at this value of θ_0 , but also to the fact that, since few propagating orders exist, the specular can grow in an interval of θ_0 between the passing-off of two consecutive propagating orders; namely, between angles of incidence at which these orders emerge at grazing angle. These effects are illustrated in Fig. 2, where the efficiencies of the averaged diffracted orders over the 200 gratings are plotted versus θ_0 . In Fig. 2 the maxima of the diffracted intensities are exactly at those θ_0 at which they become antispecular. On the other hand, the specular tends to grow at incidence angles larger than 20° , but suffers abrupt decreases whenever a passing off of a propagating order exists. This is a direct consequence of the Rayleigh anomalies at those values of θ_0 (see, e.g., Refs. 3, 15, or 16). There is a narrow interval around 45° at which the specular is the largest intensity (Fig. 2) prior to

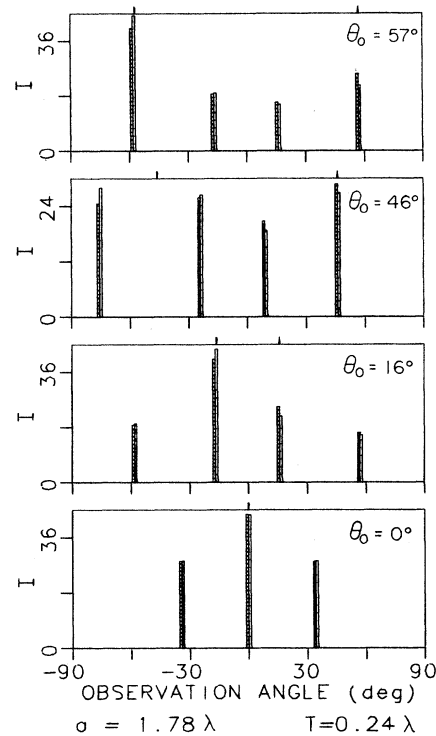


FIG. 1. Mean diffracted intensities from 200 gratings of period $a = 1.78\lambda$, at four angles of incidence $\theta_0 = 0^\circ$, 16° , 46° , and 57° , simulated from a random series with $T = 0.24\lambda$. Left bars: $\sigma = 0.5\lambda$. Right bars: $\sigma = 0.6\lambda$. Tic marks at the top: antispecular, left; specular, right.

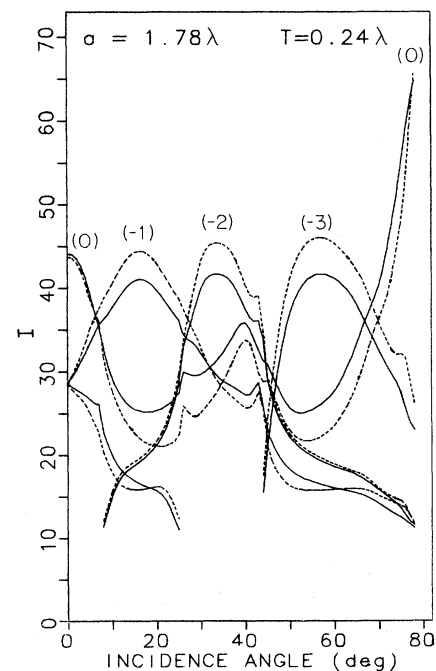


FIG. 2. Mean diffracted intensities vs incidence angle θ_0 from 200 gratings with $T = 0.24\lambda$. Solid line: $\sigma = 0.5\lambda$. Dashed line: $\sigma = 0.6\lambda$.

the appearance and growth of the order $n = -3$ that reaches its peak about $\theta_0 = 55^\circ$, where it becomes antisp specular. Also, the peaks of the antisp specular intensities are larger the greater σ is. The specular, on the other hand, grows faster the smaller the depth σ is.

The Rayleigh anomalies due to the passing off of propagating orders are associated with the prevention of the growth of the specular peak in deep gratings with a large period. Then many propagating orders are continuously appearing as θ_0 varies, so that the specular has "no room" to grow in the θ_0 diagram unless θ_0 is very large (almost grazing, in fact). This is seen in Figs. 3 and 4, which show the mean diffracted intensities at $\theta_0 = 0^\circ$, 26° , and 43° , and the efficiencies versus θ_0 for gratings with period $a = 8\lambda$, constructed from a random series with $T = 0.7\lambda$ and $\sigma = 1.2\lambda$ and 1.3λ , respectively. (In Fig. 4 only the mean efficiencies for $\sigma = 1.3\lambda$ are shown; those for $\sigma = 1.2\lambda$ are similar.) Once again, we observe that the larger σ is, the greater the enhancement of the antisp specular. For any angle θ_0 at which an antisp specular exists, the intensity of this order appears enhanced. One can see from these figures that when the period a becomes large, so that virtually every θ_0 has an antisp specular order, the corresponding intensity will appear enhanced in the backscattering direction when it is averaged over many samples. Then the envelope of mean diffracted intensities will be very close to the mean scattered intensity from a random surface.

It is remarkable that, although at those θ_0 at which there is a passing off of some order there exists a neat Rayleigh anomaly for the other mean diffracted intensities, no resulting anomaly in the θ_0 diagrams exists for those mean intensities which at that value of θ_0 grow towards a peak at which they become antisp specular. Otherwise no backscattering enhancement would occur.

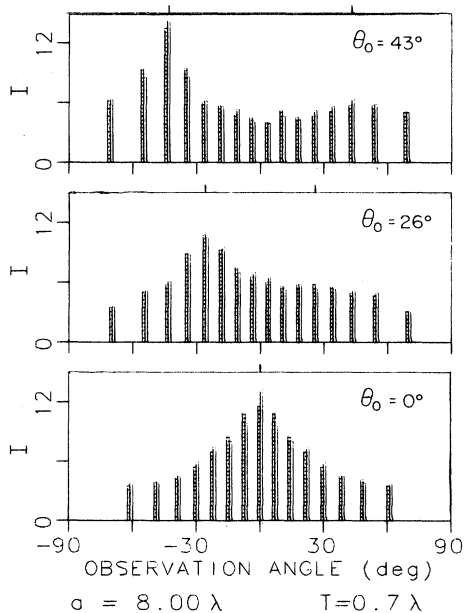


FIG. 3. Same as Fig. 1 at $\theta_0 = 0^\circ$, 26° , and 43° , $a = 8\lambda$, $T = 0.7\lambda$. Left bars: $\sigma = 1.2\lambda$. Right bars: $\sigma = 1.3\lambda$.

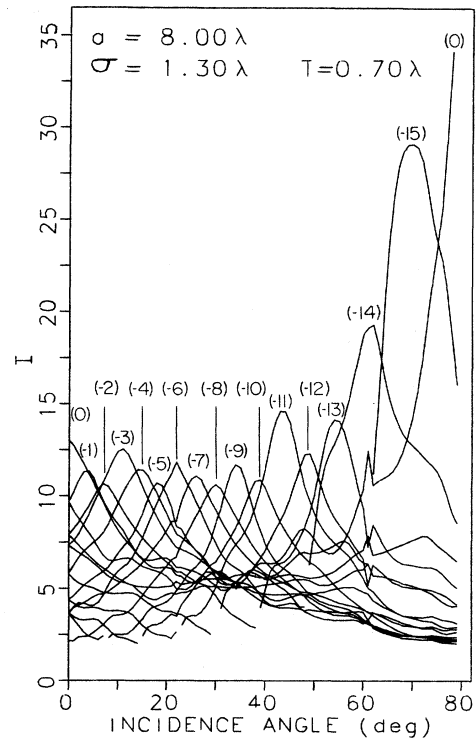


FIG. 4. Same as Fig. 2 with $a = 8\lambda$, $T = 0.7\lambda$, and $\sigma = 1.3\lambda$.

III. SYMMETRIC PROFILES

The above results are in agreement with the enhancement of the antisp specular intensities found for some particular profiles of large depth in Ref. 1. However, an enhancement of the specular was also found in that work. We are now going to show that this enhancement appears when the profile is symmetric.

Figure 5 shows the mean diffracted intensities at $\theta_0 = 0^\circ$, 26° , and 43° from 200 gratings with period $a = 8\lambda$, each of them simulated from a different interval of the same random series of $T = 0.7\lambda$ and $\sigma = 1.3\lambda$ and having subsequently introduced symmetry in the profile within the period a . As seen, the specular can be now as large as, or even stronger than, the antisp specular at any θ_0 .

Finally, by using the method established in Ref. 6, we show in Fig. 6 (solid line) the mean scattered intensity for s waves (there is not much difference in the result for p waves) for three different incidence angles $\theta_0 = 0^\circ$, 10° , and 40° for 200 samples of a random one-dimensional surface with $\sigma = 1.5\lambda$ and $T = \lambda$, having introduced symmetry in the samples. A remarkable enhancement of the specular peak (as well as of the backscattering, as expected) is seen. For comparison, the mean intensity from random samples without symmetry is depicted (dotted lines), showing the usual backscattering peak only. At T fixed, the backscattering peak increases versus the incidence angle θ_0 for two different values of σ , $\sigma = \lambda$ and 0.5λ , having been averaged, as before, over 200 random samples in which symmetry has been introduced, and with $T = \lambda$.

Figure 7 also shows that the specular increases with σ , and decreases (like the backscattering) as θ_0 increases. At very large θ_0 the specular grows further, approaching total specular reflection at grazing incidence, as expected. At $\theta_0=0^\circ$ the specular and backscattering enhancements are superimposed.

The enhancement in the specular direction from deep random surfaces, in which a center of symmetry has been introduced, can be understood by an argument equivalent to the one employed in the geometrical optics picture of Figs. 5 and 13 of Refs. 4 and 5, respectively.

Consider a wave with wave vector \mathbf{k}_0 suffering a series of scattering events according to, for example, sequence (a) [Fig. 8(a)], $\mathbf{k}_0, \mathbf{k}_1, \mathbf{k}_2, \mathbf{k}_3$, so that \mathbf{k}_1 is the wave vector after the i th scattering, and the emerging wave vector \mathbf{k}_3 is specular with respect to the incident \mathbf{k}_0 . This loop has a reversed counterpart (b): $-\mathbf{k}_3, -\mathbf{k}_2, -\mathbf{k}_1, -\mathbf{k}_0$ [Fig. 8(b)]. Due to reciprocity, the emerging waves from loop (a) and loop (b) have complex amplitudes A_a and A_b , respectively, that are equal ($A_a = A_b$). On the other hand, if loop (b) is reflected about the z axis, one obtains loop (c) [Fig. 8(c)]: $\mathbf{k}_0, \mathbf{k}'_1, \mathbf{k}'_2, \mathbf{k}'_3$. Nevertheless, since the structure is symmetric with respect to the z axis, the scattering centers 1', 2', and 3' of path (c) produce, respectively, the same scattered waves as their corresponding symmetric centers about OZ : 3, 2, and 1 of path (b), so that $A_c = A_b$; and because of the reciprocity quoted before, $A_c = A_a$. Then the coherent interference between paths (a) and (c) is constructive and yields $4|A_a|^2$, instead of $2|A_a|^2$, which would be obtained neglecting this interference. This interference produces an enhancement in the specular direction when the average over many random loops is made. The generalization of this argument to any number of scattering centers $N \geq 1$ is obvious.

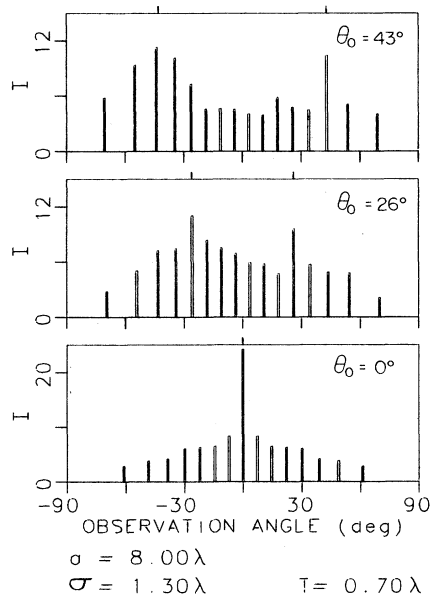


FIG. 5. Same as Fig. 1, for symmetric gratings, at $\theta_0=0^\circ, 26^\circ$, and 43° , $a=8\lambda$, $T=0.7\lambda$, $\sigma=1.3\lambda$.

The process of averaging over many samples will wash out any constructive interference due to \mathbf{k} vectors corresponding to directions other than the specular or the antiscular. In this connection, it is important to note the analogy with speckle:^{6,17} although a particular realization of a random profile can produce a speckled intensity with the maximum in a direction other than backscattering (or either backscattering or specular if symmetry exists), like a given grating can produce blaze in a certain order other than the antiscular (or either the antiscular or specular if it is symmetric), the averaging over many profiles yields the enhancements just discussed. (It is known^{6,17} that the backscattering peak is swamped by the speckle fluctuations when one considers the intensity

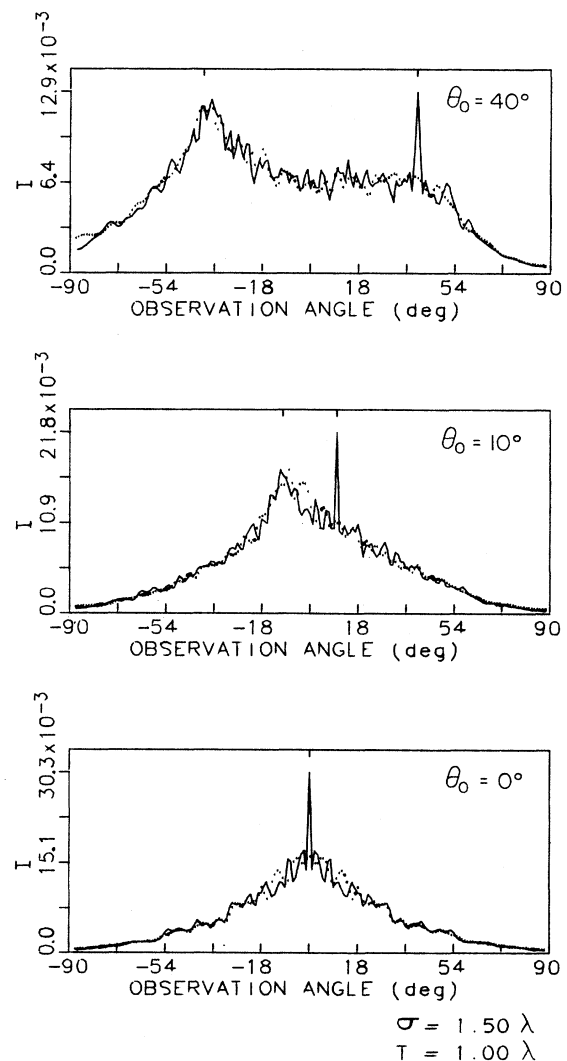


FIG. 6. Mean diffracted intensity from 200 random samples with $T=\lambda$ and $\sigma=1.5\lambda$ at three angles of incidence $\theta_0=0^\circ, 10^\circ$, and 40° . Dotted line: random samples without any symmetry. Solid line: random samples to which a center of symmetry has been introduced.

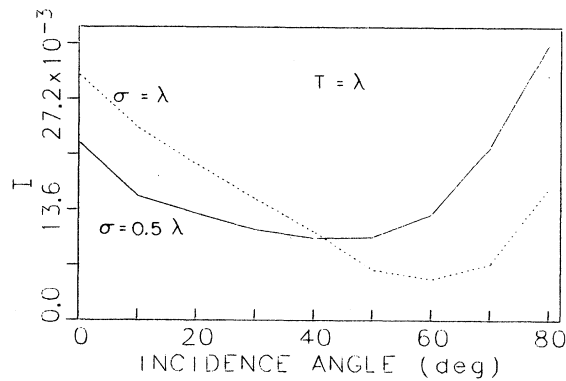


FIG. 7. Variation of the mean scattered intensity in the specular direction with the angle of incidence θ_0 , for two different depths: $\sigma = \lambda$ and $\sigma = 0.5\lambda$. $T = \lambda$. The average is done over 200 random samples to which a center of symmetry was introduced.

from a single realization of the random scatterer.)

Regarding the connection of blaze for the antispecular in reflection gratings and the enhanced backscattering from random surfaces (or the connections established for the specular in symmetric profiles), it is likely that an equivalent relationship can be established between waves reflected from volume gratings, with the periodic modulation being in the permittivity (or equivalently refractive index), and waves reflected from volumes with random permittivity.^{18,19}

Concerning transmission, although it is possible to dev-

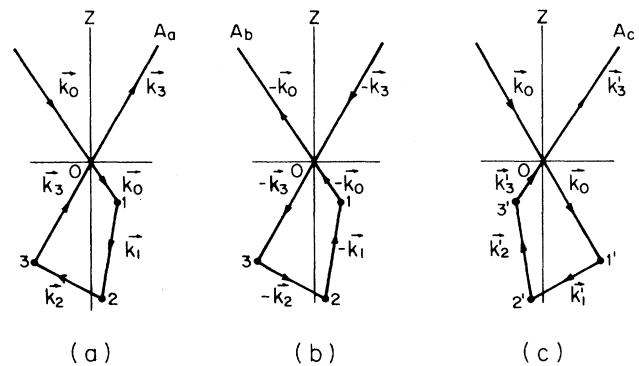


FIG. 8. Geometry used for the illustration of the specular enhancement. (a) Multiple scattering path. (b) Reciprocal path. (c) Reflection of path (b) about OZ .

ise gratings with blaze in a certain transmitted order, arguments based on reciprocity for random media, as the one used above, cannot be made.

ACKNOWLEDGMENTS

Work supported by the Comisión Interministerial de Ciencia y Tecnología (CICYT), Madrid, Spain, under Grant No. PB0278. J.M.S.-C. acknowledges a grant from Ministerio de Educación y Ciencia, Spain.

¹M. Nieto-Vesperinas and J. M. Soto-Crespo, *Phys. Rev. B* **38**, 7250 (1988).

²D. Maystre, M. Neviere, and R. Petit, in *Electromagnetic Theory of Gratings*, Vol. 22 of *Topics in Current Physics*, edited by R. Petit (Springer-Verlag, Berlin, 1980), Chap. 6.

³D. Y. Tseng, A. Hessel, and A. A. Oliner, in *Proceedings of the URSI Symposium on EM Waves* [Alta Freq. **38**, 82 (1969), special issue].

⁴E. R. Méndez and K. A. O'Donnell, *Opt. Commun.* **61**, 91 (1987).

⁵K. A. O'Donnell and E. R. Méndez, *J. Opt. Soc. Am. A* **4**, 1194 (1987).

⁶M. Nieto-Vesperinas and J. M. Soto-Crespo, *Opt. Lett.* **12**, 979 (1987).

⁷S. J. Allen, *Phys. Today* **40**(1), S-50 (1986).

⁸P. E. Wolf and G. Maret, *Phys. Rev. Lett.* **55**, 2696 (1985).

⁹E. Akkermans, P. E. Wolf, and R. Maynard, *Phys. Rev. Lett.* **56**, 1471 (1986).

¹⁰Private discussions with J. C. Dainty (Imperial College of Sci-

ence and Technology, London), A. Ishimaru (University of Washington, Seattle, WA), and A. A. Maradudin (University of California, Irvine, CA).

¹¹S. O. Rice, *Commun. Pure Appl. Math.* **4**, 351 (1951).

¹²F. Toigo, A. Marvin, V. Celli, and N. R. Hill, *Phys. Rev.* **15**, 5618 (1977).

¹³M. Nieto-Vesperinas, *J. Opt. Soc. Am.* **72**, 539 (1982); G. S. Brown, *Wave Motion* **7**, 195 (1985).

¹⁴N. García, *Opt. Commun.* **45**, 307 (1983); N. Garcia and A. A. Maradudin, *ibid.* **45**, 301 (1983).

¹⁵A. Hessel and A. A. Oliner, *Appl. Opt.* **4**, 1275 (1965).

¹⁶A. Hessel and A. A. Oliner, *Opt. Commun.* **59**, 327 (1986).

¹⁷S. Etemand, R. A. Thompson, and M. Andrejco, *Phys. Rev. Lett.* **57**, 575 (1986).

¹⁸T. K. Gaylord and M. G. Moharam, *Proc. IEEE* **73**, 894 (1985).

¹⁹M. G. Moharam and T. K. Gaylord, *J. Opt. Soc. Am.* **72**, 1385 (1982).